P H Y S I C A L   R E V I E W   L E T T E R S

Experimental Test of the Quantum Non-Gaussian Character of a Heralded Single-Photon State

Miroslav Ježek, Ivo Straka, Michal Mičuda, Miloslav Dušek, Jaromír Fiurášek, and Radim Filip

Department of Optics, Palacký University, 17. listopadu 12, 77146 Olomouc, Czech Republic
(Received 22 July 2011; published 15 November 2011)

We report on the experimental verification of quantum non-Gaussian character of a heralded single-photon state with a positive Wigner function. We unambiguously demonstrate that the generated state cannot be expressed as a mixture of Gaussian states. Sufficient information to witness the quantum non-Gaussian character is obtained from a standard photon anticorrelation measurement.

The quantum properties of light are exemplified by statistical behaviors which do not admit an explanation based on semiclassical theory. Since coherent states represent the quantum analogue of classical coherent light, a state that cannot be expressed as a convex mixture of coherent states is commonly considered to be nonclassical [1]. In particular, during recent decades nonclassical squeezed states of light have become a crucial resource for quantum optics, metrology, and quantum information processing [2,3].

Pure squeezed coherent states represent extremal points of a convex set of stochastic mixtures of Gaussian states. All such states possess a positive Wigner function and can be obtained from coherent laser beams using classical mixing and quantum interactions described by quadratic Hamiltonians. Exploiting higher-order nonlinearities involved in the photon detection process, states with negative Wigner functions can be conditionally generated from the squeezed states [4–8]. The Wigner functions of these highly nonclassical states exhibit a distinctly non-Gaussian shape. More generally, we can introduce the concept of a quantum non-Gaussian character: we say that a state exhibits a quantum non-Gaussian character if it cannot be expressed as a mixture of Gaussian states. Higher-order nonlinearities are required for preparation of such states even if they exhibit positive Wigner functions.

The famous Hudson theorem establishes an equivalence between the (quantum) non-Gaussian character and the negativity of the Wigner function for pure states [9]. However, this relation does not simply extend to mixed states [10]. Previous approaches towards the non-Gaussian character witness or measure for mixed states do not distinguish the non-Gaussian character which is compatible with a simple mixture of Gaussian states, and they also require complete information about the quantum state [11–13]. This brings a very basic and fundamental physical problem to our attention: Which mixed nonclassical quantum states with positive non-Gaussian Wigner functions do not admit explanation based solely on a stochastic non-Gaussian character? Very recently, a directly measurable witness of the quantum non-Gaussian character has been theoretically proposed [14]. The witness is based on

knowledge of probabilities of vacuum and single-photon states only, yet it can detect a wide class of states with positive Wigner functions which are not mixtures of Gaussian states.

A heralded single-photon source is an excellent example for testing the power of this witness in a laboratory. In the absence of background noise, the generated state would be a mixture of a single-photon state and a vacuum due to losses, imperfect coupling and mode matching. If the probability of a vacuum dominates, then the state exhibits a positive Wigner function. Nevertheless, the witness [14] still proves that it is not a mixture of Gaussian states. Here we apply the witness to approximate single-photon states conditionally generated by detection of an idler photon from a photon pair produced by the process of spontaneous parametric frequency down conversion (PDC). Our detection scheme consisting of a beam splitter and two single-photon detectors is the one commonly employed to test the anticorrelation properties of single-photon sources [15]. This measurement allows us to obtain suitable estimates of vacuum and single-photon probabilities, which are required for the non-Gaussian character witness. The verification of the quantum non-Gaussian character thus conveniently complements other typically performed nonclassicality tests of single-photon sources.

Theory.—Let $\mathcal{G}$ denote the set of all mixtures of Gaussian states. We would like to show that a given state ρ cannot be expressed as a convex mixture of Gaussian states, $\rho \notin \mathcal{G}$, even though ρ possesses a positive Wigner function. This can be accomplished using a criterion recently derived in Ref. [14]. This criterion is based on photon-number probabilities and can be expressed as an upper bound on a single-photon probability p_1 for a given vacuum-state probability p_0. If the measured p_1 exceeds this bound, then $\rho \notin \mathcal{G}$. The bound can be derived by maximizing p_1 for a fixed p_0 over all pure Gaussian states [14] and can be conveniently expressed in a parametric form,

$$p_0 = \frac{e^{-d^2[1-\tanh(r)]}}{\cosh(r)}, \qquad p_1 = \frac{d^2 e^{-d^2[1-\tanh(r)]}}{\cosh^3(r)}. \quad (1)$$

Here $r \geq 0$ is the squeezing constant and the displacement reads $d^2 = (e^{4r} - 1)/4$. All probability pairs (p_0, p_1)

achievable by mixtures of Gaussian states form a convex set that is shown in Fig. 1(a) as an area labeled $\mathcal{G}$. Note that the boundary of this area is specified by the formula (1).

In analogy with entanglement witnesses [16], we can define a non-Gaussian character witness [14],

$$W(a) = ap_0 + p_1. \qquad (2)$$

If $W(a) > W_G(a)$ then $\rho \notin \mathcal{G}$. The bound $W_G(a) = \max_{\rho \in G} W(a)$ can be obtained by inserting p_0 and p_1 given by Eq. (1) into Eq. (2) and maximizing the resulting expression over r. This yields the extremal equation $(1 + e^{2r})a = e^{2r}(3 - e^{2r})$ whose solution provides optimal r for any given a. As indicated by a green dashed line in Fig. 1(a), each line $ap_0 + p_1 = W_G(a)$ is a tangent to the boundary curve (1) and divides the plane into two half planes. All points (p_0, p_1) lying in the half-plane $ap_0 + p_1 > W_G(a)$ are certified by the witness to correspond to a state $\rho \notin \mathcal{G}$.

Let us now consider practical determination of the probabilities p_0 and p_1. Since the currently commonly available avalanche photodiodes (APDs) are not capable of resolving the number of photons, one needs to employ an advanced photon-number resolving detector [17–19] with demanding operation conditions or some sort of multiplexed detector [20–27]. Perhaps the conceptually simplest scheme, shown in Fig. 1(b), is based on splitting the incoming signal on a balanced beam splitter (BS) and placing an APD on each output port of the BS. This setup is commonly used for measurement of the $g^{(2)}$ factor [15,28,29].

Although this scheme provides some information about photon statistics there are several factors that need to be carefully considered. One important issue is the detector efficiency and other losses which combine to overall
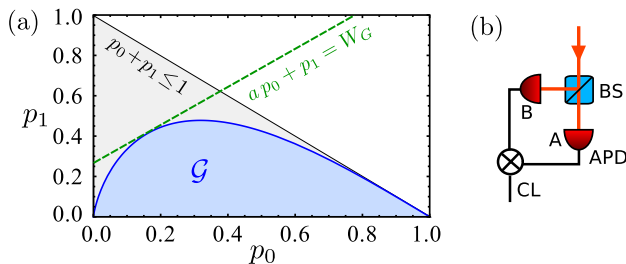
FIG. 1 (color online). (a) Inferring non-Gaussian character from photon-number probabilities p_0 and p_1 of vacuum and single-photon states. The region of physically allowed points (p_0, p_1) is formed by a triangle $p_0 + p_1 \leq 1$, $p_j \geq 0$. The convex region $\mathcal{G}$ represents probability pairs achievable by mixtures of Gaussian states. The points lying in the light gray region indicate states that cannot be expressed as convex mixtures of Gaussian states. The green dashed line represents one of the non-Gaussian character witnesses $W(a)$. (b) Detection scheme. Signal light beam impinges on a beam splitter (BS) and the outputs are detected by two APDs. Both single and coincidence rates are acquired by coincidence logic (CL).

efficiency η. Compensation of η would require its precise calibration, which is a nontrivial task. However, we can simply include losses into state preparation. Let L_η denote a lossy channel with transmittance η. This channel maps Gaussian states onto Gaussian states. Therefore, if $\rho \in \mathcal{G}$ then also $\rho_\eta \equiv L_\eta[\rho] \in \mathcal{G}$. This implies that if $\rho_\eta \notin \mathcal{G}$ then also $\rho \notin \mathcal{G}$. We can thus conservatively assume perfect detectors with unit efficiency and if $\rho_\eta \notin \mathcal{G}$ is proven under this assumption, then it certainly holds also for ρ irrespective of the exact value of η.

In the experiment, the number of single detector clicks (R_{1A} and R_{1B}) as well as the number of coincidence clicks (R_2) is measured for a given number of samples R_0 of the state. Assuming perfect detectors with $\eta = 1$ the vacuum-state fraction p_0 is the probability that none of the detectors clicks,

$$p_0 = 1 - \frac{R_{1A} + R_{1B} + R_2}{R_0}. \qquad (3)$$

The determination of p_1 is less trivial. We have

$$\frac{R_{1A}}{R_0} = \sum_{n=1}^{\infty} T^n p_n, \qquad \frac{R_{1B}}{R_0} = \sum_{n=1}^{\infty} (1 - T)^n p_n, \qquad (4)$$

where T denotes the effective transmittance of the BS that also includes possible imbalance of the detection efficiencies and other factors. Note that R_{1A} and R_{1B} depend on the whole photon-number distribution p_n, not just on p_0 and p_1. We can nevertheless construct the following estimator,

$$p_{1,\text{est}} = \frac{R_{1A} + R_{1B}}{R_0} - \frac{T^2 + (1 - T)^2}{2T(1 - T)} \frac{R_2}{R_0}. \qquad (5)$$

With the help of Eqs. (3) and (4) one can show that

$$p_{1,\text{est}} = p_1 - \sum_{n=3}^{\infty} p_n \frac{T^2 - T^n + (1 - T)^2 - (1 - T)^n}{2T(1 - T)},$$

hence $p_{1,\text{est}} \leq p_1$. Note that the term proportional to p_2 is absent in $p_{1,\text{est}}$, so for rapidly decaying distributions the error is of the order of p_3. With this lower bound on p_1 at hand, the above criterion is still applicable, because $ap_0 + p_{1,\text{est}} > W_G(a)$ implies that $ap_0 + p_1 > W_G(a)$ as well.

The estimation of p_1 is influenced by the effective imbalance of the detection channels $T : (1 - T)$. Without loss of generality, we can assume that $T > \frac{1}{2}$. It follows from Eq. (5) that $p_{1,\text{est}}$ decreases with increasing ratio $T : (1 - T)$. Hence we should avoid underestimation of T which would result in overestimation of p_1. An upper bound on T is provided by the ratio of single detector clicks,

$$T_{\text{est}} = \frac{R_{1A}}{R_{1A} + R_{1B}}. \qquad (6)$$

It can be shown that $T \leq T_{\text{est}}$ for $T \geq \frac{1}{2}$. We can thus safely use T_{est} as a conservative estimate of T.

Multiple witness.—Many single-photon sources do not emit photons strictly into a single spatial and temporal mode. Let us briefly sketch a proof [30] of the applicability of the witness to a generic multimode case. Let N denote the total number of modes involved, and we define the total photon-number $n = \sum_{j=1}^{N} n_j$, where n_j is the number of photons in jth mode. The estimated probabilities p_n then correspond to the probability of no photon ($n = 0$) or one photon in total ($n = 1$) in the signal beam. Even in this multimode case, the maximum of $W(a) = ap_0 + p_1$ over all mixtures of Gaussian states is attained by a pure N-mode Gaussian state. Any N-mode pure Gaussian state can be prepared by combining N single-mode squeezed states in a network of beam splitters. Moreover, the passive linear network described by a unitary matrix U_N does not change the statistics of the total photon-number because $U_N n U_N^\dagger = n$. It suffices to carry out the optimization over products of N pure single-mode Gaussian states which can be done analytically and one can prove that the bound on $W(a)$ remains $W_G(a)$ for arbitrary N. We can therefore apply the witness also to multimode states without any limitation.

Experimental setup.— The experimental setup of a heralded single-photon source based on PDC is presented in Fig. 2. The detection part consists of three binary detectors (TR, SA, SB). The trigger detector (TR) yields a heralding
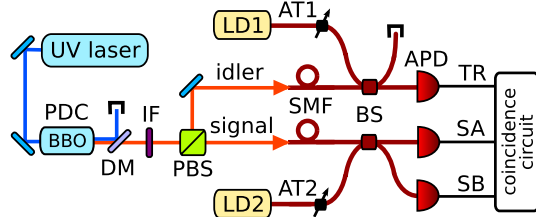
FIG. 2 (color online). Layout of the experimental setup. Continuous-wave frequency-multimode ultraviolet laser with central wavelength of 407 nm pumps a 2 mm long β-barium borate (BBO) nonlinear crystal phase matched for type 2 degenerate PDC. Collinearly generated photon pairs with central wavelength of 814 nm are collimated and separated from the pump beam by a dichroic mirror (DM) and spectrally limited by an interference filter (IF) to 10 nm. The orthogonally polarized photons of a PDC pair are separated by a polarizing beam splitter (PBS) and coupled to single-mode optical fibers (SMF). Both outputs can be mixed with an attenuated (AT) infrared laser diode (LD) signal at fiber beam splitters (BS) to emulate dark counts of detectors and a noise component of the explored quantum state. The three output modes are then detected by binary single-photon detectors based on silicon avalanche photodiodes (APD) operated in Geiger mode and actively quenched. The absolute quantum efficiency of the detectors is specified by a manufacturer to approximately 50%, while their relative efficiencies were precisely measured prior to the experiment and found to be 100%, $91.7 \pm 0.2\%$, $92.2 \pm 0.2\%$ for TR, SA, SB channels, respectively. Electronic dark counts of the detectors in coincidence basis were found to be completely negligible.

output of the single-photon PDC source. When a detection event is registered at this detector, we expect that an approximate single-photon state is prepared in signal mode. The signal is divided by the BS with transmittance of $T_{BS} = 0.522 \pm 0.003$ to the detection channels SA and SB. All single as well as twofold and threefold coincidence events between channels TR, SA, and SB are registered by a fast coincidence logic unit. The overall splitting ratio T_{est} between channels SA and SB has been conservatively estimated from the measured rates R_{1A} and R_{1B} using Eq. (6), and it agrees well with the independently measured T_{BS} and relative detector efficiencies.

The probabilities p_0 and p_1 are estimated from the measured data using formulas (3) and (5). Because of conditioning on clicks of the trigger, R_0 is given by the singles of the trigger detector, R_{1A} and R_{1B} by twofold coincidences of TR&SA and TR&SB, respectively, while R_2 is actually given by the threefold coincidences. The coincidence window is set to 2 ns. The results are summarized in Table I for different pump powers P and three different full width at half maximum of the interference filter (IF) (2 nm, 10 nm and without filter). Because of imperfect mode-matching, incoupling losses, and inefficient detectors, the vacuum term p_0 dominates while the single-photon fraction is below 30% for all data shown. The contribution of higher photon terms is very small, $1 - p_0 - p_1 \lesssim 10^{-4}$, so the generated state is very close to an attenuated single photon. In the experiment, this is indicated by a very small ratio of threefold to twofold coincidence rates (less than 10^{-3}). For example, for $P = 50$ mW and $w = 10$ nm we have $R_2 = 605$, $R_{1A} = 1.259 \times 10^6$, and $R_{1B} = 1.192 \times 10^6$ per 100 s. The statistical uncertainty of the estimated p_0 and p_1 determined assuming Poissonian statistics is less than 2×10^{-4} for all data shown (1 standard deviation). Because of very low threefold coincidences, the sum $p_0 + p_1$ exhibits much lower statistical uncertainty than the difference $p_0 - p_1$.

Results.—We have verified that the generated states cannot be expressed as a mixture of Gaussian states by using the non-Gaussian character witness. For each data set (p_0, p_1) we have calculated $\Delta W = ap_0 + p_1 - W_G(a)$ and maximized the difference over all a. The resulting maximal ΔW values are listed in Table I. We can see that $\Delta W > 0$ in all cases and the bound $W_G(a)$ is always

TABLE I. Estimated probabilities p_0 and p_1, and the corresponding witness ΔW are shown for several different pump powers P and IF widths w ($\cdots$ denotes no filter).

P [mW]	w [nm]	p_0	p_1	$\Delta W[\times 10^{-6}]$
50	2	0.9124	0.0875	412 ± 1
50	10	0.8589	0.1410	1666 ± 3
20	10	0.8425	0.1574	2370 ± 2
50	$\cdots$	0.7095	0.2901	$14\,252 \pm 17$
5	$\cdots$	0.7296	0.2704	$11\,825 \pm 15$

TABLE II.   The same as Table I, n_{rel} indicates the amount of noise injected from LD1 and LD2 into trigger and signal detectors, $P = 50$ mW, and IF width $w = 10$ nm.

n_{rel}	p_0	p_1	a_{opt}	$\Delta W[\times 10^{-6}]$
0.0	0.8195	0.1804	0.940 18	3479 ± 7
0.1	0.9073	0.0926	0.983 89	406 ± 3
0.2	0.9408	0.0591	0.993 32	42 ± 2
1.0	0.9777	0.0222	0.999 03	-84 ± 1

FIG. 3 (color online).   The multiphoton contribution $1 - p_0 - p_1$ is plotted as a function of p_1. Symbols indicate experimental data for several different levels of noise added simultaneously by LD1 and LD2 (red squares) and by LD1 only (green circles). All other parameters were fixed, $P = 50$ mW and $w = 10$ nm. Error bars stand for 3 standard deviations, horizontal error bars of p_1 are smaller than the size of the symbols. The solid blue curve represents the boundary given by Eq. (1), all points to the right of this curve correspond to states that cannot be obtained as mixtures of Gaussian states.

surpassed by many standard deviations. Next, we investigate the influence of background noise on the source properties. For this purpose we inject light from laser diodes LD1 and LD2 into trigger and signal detection blocks, respectively. Noise from LD2 emulates background noise of the source while noise coming from LD1 effectively increases dark count rate of the trigger thus increasing the vacuum fraction p_0. Table II shows the results obtained when the amount of injected noise is the same in both blocks and n_{rel} indicates the normalized noise strength. With increasing noise we can clearly observe transition to the regime where $\Delta W < 0$, as is also illustrated in Fig. 3.

Discussion.—Let us briefly compare our results with other nonclassicality measures. Since $p_0 > 0.5$ for all the measured states (cf. Tables I and II and Fig. 3), their Wigner function is always positive in the origin, $W(0) = \frac{1}{\pi}\langle(-1)^n\rangle \geq \frac{2p_0-1}{\pi} > 0$, where it is expected to exhibit maximum negativity $W(0) = -\frac{1}{\pi}$ for a pure single-photon state [31]. On the other hand, all the measured states cannot be expressed as a mixture of coherent states, therefore they are nonclassical [32]. The nonclassicality can be quantified by a $g^{(2)}$ parameter defined as $g^{(2)}(0) = \frac{\langle a^{\dagger 2} a^2 \rangle}{\langle a^\dagger a \rangle^2}$ [33]. Sub-Poissonian photon-number statistics is indicated by $g^{(2)}(0) < 1$. The state produced by our source can be excellently approximated by a density matrix $\rho_T = p_0|0\rangle\langle 0| + p_1|1\rangle\langle 1| + (1 - p_0 - p_1)|2\rangle\langle 2|$ because higher photon terms are exponentially suppressed due to very low parametric gain in the nonlinear crystal. In this case we find $g^{(2)}(0) = \frac{2(1-p_1-p_0)}{[2(1-p_0)-p_1]^2}$ yielding $g^{(2)}(0) < 0.3661$ for all states. Simultaneously, all the results exhibit a very strong photon anticorrelation effect, witnessed by $\alpha = \frac{R_0 R_2}{R_{1A} R_{1B}} < 0.3706$ which violates the classical inequality $\alpha \geq 1$ [15]. The limits are given by data for $n_{rel} = 1$ in Table II and Fig. 3. All the above parameters are monotonically decreasing as less noise is imposed by LD1 and LD2 and for $n_{rel} = 0.2$ we already have $\alpha = 0.0521$ and $g^{(2)}(0) = 0.0519$.

In conclusion, we have examined a source producing approximate single-photon states with a positive Wigner function but exhibiting strong photon anticorrelation and we have unambiguously proved that the generated states cannot be expressed as mixtures of Gaussian states. In

comparison to the witness based on negativity of the Wigner function [31], the present criterion can identify a high nonclassicality of a much wider class of single-photon sources, while avoiding the need for demanding estimation of complete photon-number distribution or complicated data processing [34]. Consequently, the presented criterion is particularly useful for evaluation of single-photon sources where negativity of the Wigner function cannot be observed [35].

[1] R. Glauber, *Quantum Theory of Optical Coherence* (Wiley-VCH, Weinheim, 2007).

[2] H.-A. Bachor and T. C. Ralph, *A Guide to Experiments in Quantum Optics* (Wiley-VCH, Weinheim, 2004).

[3] A. Furusawa and P. van Loock, *Quantum Teleportation and Entanglement: A Hybrid Approach to Optical Quantum Information Processing* (Wiley-VCH, Weinheim, 2011).

[4] A. I. Lvovsky, H. Hansen, T. Aichele, O. Benson, J. Mlynek, and S. Schiller, Phys. Rev. Lett. **87**, 050402 (2001).

[5] A. Zavatta, S. Viciani, and M. Bellini, Science **306**, 660 (2004).

[6] A. Ourjoumtsev, R. Tualle-Brouri, J. Laurat, and Ph. Grangier, Science **312**, 83 (2006).

[7] J. S. Neergaard-Nielsen, B. M. Nielsen, C. Hettich, K. Molmer, and E. S. Polzik, Phys. Rev. Lett. **97**, 083604 (2006).

[8] K. Wakui, H. Takahashi, A. Furusawa, and M. Sasaki, Opt. Express **15**, 3568 (2007).

[9] R. L. Hudson, Rep. Math. Phys. **6**, 249 (1974).

[10] A. Mandilara, E. Karpov, and N. J. Cerf, Phys. Rev. A **79**, 062302 (2009).

[11] V. V. Dodonov, O. Manko, V. Manko, and A. Wunsche, J. Mod. Opt. **47**, 633 (2000).

[12] M. G. Genoni, M. G. A. Paris, and K. Banaszek, Phys. Rev. A **78**, 060303(R) (2008).

[13] M. Barbieri, N. Spagnolo, M. G. Genoni, F. Ferreyrol, R. Blandino, M. G. A. Paris, P. Grangier, and R. Tualle-Brouri, Phys. Rev. A **82**, 063833 (2010).

[14] R. Filip and L. Mišta, Jr., Phys. Rev. Lett. **106**, 200401 (2011).

[15] P. Grangier, G. Roger, and A. Aspect, Europhys. Lett. **1**, 173 (1986).

[16] M. Lewenstein, B. Kraus, J. I. Cirac, and P. Horodecki, Phys. Rev. A **62**, 052310 (2000).

[17] J. Kim, S. Takeuchi, Y. Yamamoto, and H. H. Hogue, Appl. Phys. Lett. **74**, 902 (1999).

[18] A. E. Lita, A. J. Miller, and S. W. Nam, Opt. Express **16**, 3032 (2008).

[19] B. E. Kardyna, Z. L. Yuan, and A. J. Shields, Nat. Photon. **2**, 425 (2008).

[20] H. Paul, P. Törmä, T. Kiss, and I. Jex, Phys. Rev. Lett. **76**, 2464 (1996).

[21] K. Banaszek and I. A. Walmsley, Opt. Lett. **28**, 52 (2003).

[22] J. Řeháček, Z. Hradil, O. Haderka, J. Peřina, Jr., and M. Hamar, Phys. Rev. A **67**, 061801 (2003).

[23] D. Achilles, C. Silberhorn, C. Śliwa, K. Banaszek, and I. A. Walmsley, Opt. Lett. **28**, 2387 (2003).

[24] M. J. Fitch, B. C. Jacobs, T. B. Pittman, and J. D. Franson, Phys. Rev. A **68**, 043814 (2003).

[25] M. Mičuda, O. Haderka, and M. Ježek, Phys. Rev. A **78**, 025804 (2008).

[26] M. Avenhaus, K. Laiho, M. V. Chekhova, and C. Silberhorn, Phys. Rev. Lett. **104**, 063602 (2010).

[27] D. A. Kalashnikov, S. H. Tan, M. V. Chekhova, and L. A. Krivitsky, Opt. Express **19**, 9352 (2011).

[28] E. Bocquillon, C. Couteau, M. Razavi, R. Laflamme, and G. Weihs, Phys. Rev. A **79**, 035801 (2009).

[29] D. Höckel, L. Koch, and O. Benson, Phys. Rev. A **83**, 013802 (2011).

[30] R. Filip and F. Grosshans (to be published).

[31] K. Laiho, K. N. Cassemiro, D. Gross, and C. Silberhorn, Phys. Rev. Lett. **105**, 253603 (2010).

[32] L. Lachman and R. Filip (to be published); using the same structure of the witness, the nonclassicality witness can be expressed as $W(a) > e^{a-1}/(1 + a)$.

[33] R. Loudon, *The Quantum Theory of Light* (Oxford University Press, Oxford, 2000) p. 245 3rd ed..

[34] A. Mari, K. Kieling, B. M. Nielsen, E. S. Polzik, and J. Eisert, Phys. Rev. Lett. **106**, 010403 (2011).

[35] For a recent review, see: S. Scheel, J. Mod. Opt. **56**, 141 (2009).